IEEE Access
Multidisciplinary | Rapid Review | Open Access Journal

Received October 9, 2018, accepted November 1, 2018, date of publication November 12, 2018,
date of current version December 18, 2018.

Digital Object Identifier 10.1109/ACCESS.2018.2880191

A High Efficiency Power Amplifier Method Using Signal Decomposition in OFDM Communication System

ZHIYUAN REN, ZEHUAN HU, AND HAILIN ZHANG, (Member, IEEE)
State Key Laboratory of Integrated Services Network, Xidian University, Xi'an 710071, China

Corresponding author: Zhiyuan Ren (zyren@s-an.org)

This work was supported in part by the National Key Research and Development Program of China under Grant 2016YFE0123000, in part by the National Natural Science Foundation of China under Grant 61201133, Grant 61571338, Grant 61671347, Grant 61572389, and Grant 61620106011, in part by the National Key Research and Development Program of China under Grant SQ2016YFHZ021501, in part by the Key Research and Development Plan of Shaanxi Province under Grant 2017ZDCXL-GY-05-01, and in part by the 111 Project in Xidian University of China under Grant B08038.

ABSTRACT OFDM is a powerful competitive technology in the 5G era and is one of the core technologies in 4G communication system, due to its robust to multipath-fading and high frequency efficiency. However, the high peak-to-average-power-rate (PAPR) problem of OFDM has not been fully solved, which should be considered specifically in 5G communication system, and it is harmful to the power efficiency of power amplifier. For the purpose of alleviating high PAPR problem, in this paper, a signal decomposition scheme is introduced into the high PAPR OFDM system. With the method, the original signal is decomposed into multi-branched signals which will be amplified by multi power amplifiers, and then the amplified signals are combined for transmission. After decomposition, all of the branched signals have lower PAPR, which significantly increase the power efficiency of branched power amplifier. Both of the theoretical analysis and simulation results indicate that the performance of PAPR and power efficiency can be improved.

INDEX TERMS OFDM, power amplifier, signal decompose, PAPR.

I. INTRODUCTION

Nowadays, the fifth generation communication system (5G) has been researched widely, which will increase the capacity 100-1000 times than the fourth generation (4G) [1]–[3]. Hence, to meet the requirement of high data rate and capacity, the multi-carrier modulation schemes, namely Orthogonal Frequency Division Multiplexing (OFDM), have been widely used in many high-speed communication systems, for instance, IEEE 802.11a/g/n/ac, IEEE 802.16 (WiMAX), Asymmetric Digital Subscriber Line (ADSL), Digital Audio Broadcasting (DAB) and Digital Video Broadcasting-Terrestrial (DVB-T) [4]–[6]. OFDM has already played an important role in the 4G LTE/LTE-A standards because of its high spectral efficiency, immunity of Inter-Symbol Interference (ISI) and robustness of multi-path channel fading. Besides, OFDM is a good candidate for 5G communication systems [7]. However, its high peak-to-average-power ratio (PAPR) problem has not been fully solved. Since peak signals cannot be predicted, saturated distortion will occur if power amplifier (PA) cannot accommodate to the envelope of the peak signals. This will result in the increases of Bit Error Rate (BER) as well as out-of-band radiation at the receiver. Although this problem can be solved by adopting PA with large Output Power Back Off (OBO), energy waste and lower power efficiency are inevitable. An alternative way is to use a high-cost wide range power amplifier (WR-PA) to accommodate the peak signal. However, as other signals are far smaller than the peak signals, this approach also degrades the power efficiency severely. Therefore, how to increase the power efficiency of PA for OFDM system has gained much attention recently.

Aiming at these problems, many studies have been developed, such as Clipping, Selected Mapping (SLM) and Precoded OFDM method etc. [8]–[14]. Among these studies, Clipping was the earliest proposed method which simply clipped the peak signals directly. Clipping would seriously decrease the BER performance at the receiver, hence it is rarely used in reality. SLM would be classified as none-distortion PAPR reduction methods, but the side information need to be transmitted with signals, which decreases the

performance of data transmission [8]–[11]. Precoded OFDM method has the advantage of efficiency and reliability, but the computational complexity problem cannot be solved perfectly [12]–[16]. Paper [14] proposes a novel precoded system, which reduces both of the computational complexity and the PAPR by using a Walsh-Hadamard matrix to perform the precoding operation, but it still needs the inverse matrix in the receiver to restore the original signals. Specifically, in the standard of LTE/LTE-A uplink, the Discrete Fourier Transform (DFT) matrix is adopted to be the precoded matrix, and the resulting system becomes a single-carrier system, i.e., Single Carrier Frequency Domain Equalization (SC-FDE). But SC-FDE sacrifices the orthogonality for lower PAPR. In paper [17], a segmented power generation (SPG) method based on multiple amplifier structure is proposed to improve the efficiency and linear performance of amplifiers. However, the SPG method cannot decrease the PAPR of OFDM signals. Tone injection, a kind of probability technologies, is another method for PAPR reduction [18]–[20]. Probability technology reduces the probability of high PAPR,and generates sideband information, which leads to the decrease of system throughput [21]. In terms of signal decomposition methods, paper [22] proposes the signal decomposition technique as one of solution to mitigate the large PAPR to be addressed in OFDM transmitters. The technique mainly focuses on enhancing the receiver SNR, and it improves the PAPR indeed. However, those two methods [21], [22] are not good enough to reduce PAPR.

In order to solve the high PAPR and low power efficiency problem, based on multi PA structure we have preliminarily studied a Signal Decomposed Power Amplifier (SDPA) method in our related work, i.e. Symmetric Uniform SDPA (SUSDPA) [23]. The SDPA method decomposes the high PAPR signal into multiple branched-signals, where the peak power of each branched-signal are less than that of original signal. It means that the PAPR of branched-signals are decreased. Since the branched-signals of SDPA have the advantages of low peak power and low PAPR, the power efficiency of branched-PA could also be improved, which satisfies the requirement of Green Radio [24], [25]. In this paper, we will further deduce the PAPR reduction result theoretically, and the power efficiency will be analyzed too. The remainder of this paper will be arranged as follows: section II will introduce the system model and some conclusions which will be used for analysis. Section III will propose the scheme of SUSDPA, and the result will be demonstrated by simulation in section IV. In section V, we will conclude the paper.

II. BACKGROUND

A. SYSTEM MODEL

Fig. 1 shows the basic structure of OFDM system. The input baseband signal of PA, i.e., x, is the original vector signal. The instantaneous signal of x is denoted as $x(t)$. Since OFDM has the characteristic of high PAPR, $x(t)$ may be larger than the linear range of the PA, or even saturation point, which

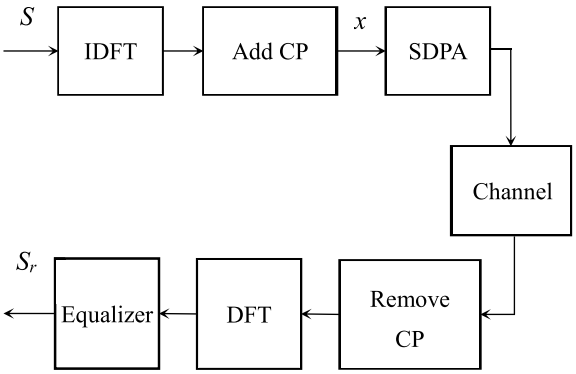

FIGURE 1. The structure of OFDM.

significantly decrease the BER performance. In this paper, a signal decomposed method is proposed to decrease the influence of high PAPR signal and to improve the power efficiency.

1) THE ARCHITECTURE OF SDPA

The framework of SDPA is given in Fig. 2, where x is the high PAPR original signal. The original vector signal x will be decomposed into multi-branches signals $x_1, x_2, \ldots, x_n$, where x_i represents the ith branched-signal. Those branched-signals will be amplified by multi branched-PAs, and then combined for transmission.

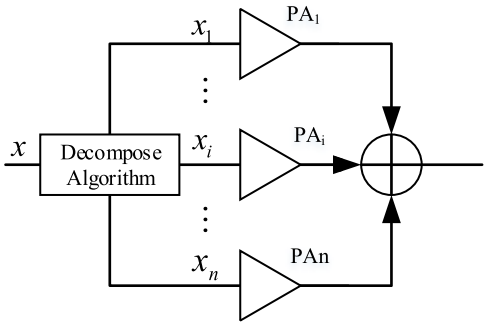

FIGURE 2. The structure of SDPA.

As Fig. 2 shows, x and x_i satisfy the following conditions:

$$\begin{cases} \sum_{i=1}^{n} x_i = x, \\ \sum_{i=1}^{n} |x_i|^2 = |x|^2. \end{cases} \tag{1}$$

The first equation of Eqs. (1) is to ensure the equality between the summation of the synthetic branched-signals and the original signal, meaning that our decomposition will not cause signal distortion. The function of the second one is to guarantee the invariance of the average signal power before and after the decomposition, which accords with energy conservation completely. For simplicity, we can introduce a new parameter η_i, and assume $x_i = \eta_i x$. Based on Eqs. (1), η_i must

satisfy:

$$\begin{cases} \sum_{i=1}^{n} \eta_i = 1, \\ \sum_{i=1}^{n} |\eta_i|^2 = 1. \end{cases} \tag{2}$$

Many sets of η_i can satisfy Eqs. (2), and different group means different decomposed algorithm. In section III, we will introduce one kind of decomposed algorithms and it will remarkably decrease the influence of high PAPR signal.

B. THE MODEL OF POWER AMPLIFIER

PA is one of the key parts in communication system. However, it has the problems of nonlinear distortion and saturation distortion, which influence the system performance remarkably in high PAPR system. Generally speaking, the amplifier linearization technology can be implemented on each branch to eliminate the nonlinear distortion of branched-PA. Detailed researches of linearization techniques under various conditions have been conducted in [26]–[29]. Hence, in this paper the amplifier will not cause any nonlinear distortion. Thus, a linear amplifier model is employed in this section, whose formulation is given in Eq. (3), as Fig. 3 shows:

$$q(t) = \begin{cases} \sqrt{G}r(t) & r(t) < V \\ \sqrt{G}V & r(t) \geq V \end{cases} \tag{3}$$

where $r(t)$ and $q(t)$ denote the amplitudes of the instantaneous input baseband signal $x(t)$ and output signal of PA respectively. G represents the power gain, and V represents the saturation amplitude of PA, which means V^2 is the saturation power.

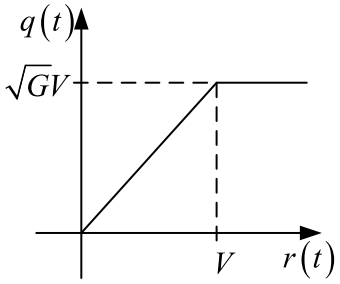

FIGURE 3. The model of PA.

C. OFDM SIGNAL DISTRIBUTION CHARACTERISTIC

We assume the number of subcarriers will be N in OFDM system. As is known to all, both of the real and imaginary part of OFDM obey approximately Gaussian distribution for large N with mean zero. Based on these conditions, we could give some lemmas as follows.

Lemma 1: Let $P(r_a, r_b)$ indicates the probability of the OFDM signals whose amplitude are within the interval $[r_a, r_b]$. There is

$$P(r_a, r_b) = exp(\frac{-r_a^2}{2\sigma^2}) - exp(\frac{-r_b^2}{2\sigma^2}). \tag{4}$$

Proof: The amplitude of the OFDM signals obeys Rayleigh distribution. Therefore, the Probability Density Function (PDF) of amplitude r, i.e., $p(r)$, can be expressed as

$$p(r) = \frac{r}{\sigma^2} exp(\frac{-r^2}{2\sigma^2}), \tag{5}$$

where $2\sigma^2$ is the mean power of OFDM signal. Then, the probability of the OFDM signals whose amplitude are within the interval $[r_a, r_b]$ could be deduced as

$$P(r_a, r_b) = \int_{r_a}^{r_b} p(r)dr = exp(\frac{-r_a^2}{2\sigma^2}) - exp(\frac{-r_b^2}{2\sigma^2}). \tag{6}$$

Lemma 2:. Let $POW(r_a, r_b)$ indicates the average power of the OFDM signals whose amplitudes are within the interval $[r_a, r_b]$, as Fig. 4 shows. There is

$$POW(r_a, r_b) = (r_a^2 + 2\sigma^2)exp(\frac{-r_a^2}{2\sigma^2}) - (r_b^2 + 2\sigma^2)exp(\frac{-r_b^2}{2\sigma^2}). \tag{7}$$

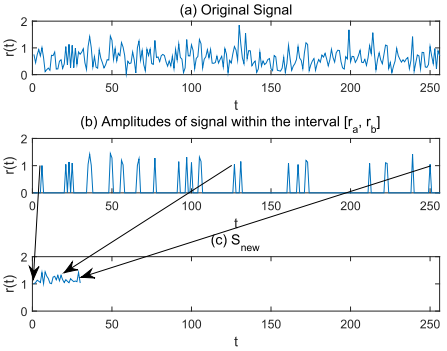

FIGURE 4. Comparison of signals within the interval $[r_a, r_b] = [1, 2]$.

Proof: Since the amplitudes of OFDM signals obey Rayleigh distribution, we can acquire the power distribution of OFDM signals. The average power of OFDM signal can be calculated by using the PDF as

$$\begin{aligned} POW(r_a, r_b) &= \int_{r_a}^{r_b} r^2 p(r)dr \\ &= (r_a^2 + 2\sigma^2)exp(\frac{-r_a^2}{2\sigma^2}) \\ &\quad -(r_b^2 + 2\sigma^2)exp(\frac{-r_b^2}{2\sigma^2}). \end{aligned} \tag{8}$$

Lemma 3: For any OFDM signal, if we could pick those signals whose amplitude within the interval $[r_a, r_b]$ to form a new signal S_{new}, as Fig.4(c) shows, the mean power of new signal S_{new} is

$$POW(S_{new}) = \frac{POW(r_a, r_b)}{P(r_a, r_b)}. \tag{9}$$

Proof: Obviously S_{new} no longer obeys the distribution of typical OFDM characteristic. After we form the new signal,

the probability of the amplitude of S_{new} changes to $P(r|r_a < r < r_b)$. Therefore,

$$P(r|r_a < r < r_b) = \frac{P(r)}{P(r_a < r < r_b)}. \tag{10}$$

Since $P(r_a < r < r_b) = P(r_a, r_b)$ is constant, taking the derivative of $P(r)$ with respect to r in Eq.(10), we can obtain the probability density function, i.e., $p(r|r_a < r < r_b)$, of S_{new} as follow

$$p(r|r_a < r < r_b) = \frac{p(r)}{P(r_a < r < r_b)}. \tag{11}$$

Substituting Eq. (11) into Eq. (8), we have

$$\begin{aligned} POW(S_{new}) &= \int_{r_a}^{r_b} r^2 p(r|r_a < r < r_b) dr \\ &= \int_{r_a}^{r_b} \frac{r^2 p(r)}{P(r_a < r < r_b)} d(r) \\ &= \frac{POW(r_a, r_b)}{P(r_a, r_b)}. \end{aligned} \tag{12}$$

Lemma 4: Let $\delta(S_{new})$ indicates the power efficiency of PA when the input signal changes to S_{new}, and it can be expressed as

$$\delta(S_{new}) = \frac{POW(r_a, r_b)}{2V^2 P(r_a, r_b)}. \tag{13}$$

Proof: According to [30], with the idealized transistor device model, the average power efficiency depends on the PA class. In this paper, we choose class A to study the power efficiency because of the simplicity. Therefore, the average power efficiency [30], [31] can be described as

$$\delta = \delta_A = E(\delta(t)) = \frac{E(r(t)^2)}{2P_v}, \tag{14}$$

where $r(t)$ is the amplitude of signal $x(t)$, $E\{\cdot\}$ denotes the statistical averaging, $P_v = V^2$ and V indicate the saturation power and the saturation amplitude PA respectively.

Based on Eq. (8), we could know that the average power of OFDM signals whose amplitude are within the interval $[r_a, r_b]$ is

$$E(r(t)^2) = POW(r_a, r_b). \tag{15}$$

Substituting Eq. (15) into Eq. (14), $\delta(r_a, r_b)$ can be expressed as

$$\delta(r_a, r_b) = \frac{POW(r_a, r_b)}{2V^2}. \tag{16}$$

When the input signal changes to S_{new}, based on Eq. (12), Eq. (16) would be deduced as

$$\delta(S_{new}) = \frac{POW(S_{new})}{2V^2} = \frac{POW(r_a, r_b)}{2V^2 P(r_a, r_b)}. \tag{17}$$

Combining Eqs. (4), (7) and (13), the OFDM signals can be discussed in different intervals, which facilitates the theoretical analysis of the following works.

The symbols which we use in this paper are arranged as Table 1 below.

TABLE 1. Symbol list.

symbol	meaning
N	The number of OFDM symbol
n	The number of branched-signals
x	Original signals
x_i	The ith branched signals
$x(t)$	The instantaneous signal of x
η_i	The ratio of x_i and x
r	The amplitude of original signal x
T	T belongs to the OFDM symbol duration.
$r(T)$	The amplitudes of instantaneous signal $x(t)$
$q(t)$	The amplitudes of the instantaneous PA output signal
G	Power Gain
V	Saturation amplitude of PA
V^2	Saturation power of PA
$2\sigma^2$	The average power of OFDM signal
$p(r)$	The probability density function of r
$\delta(t)$	instantaneous power efficiency of PA
δ	power efficiency of PA
$P(r_a, r_b)$	The probability of the OFDM signals whose amplitude are within the interval $[r_a, r_b]$
$POW(r_a, r_b)$	The average power of the OFDM signals whose amplitudes are within the interval $[r_a, r_b]$
$\delta(r_a, r_b)$	The power efficiency of PA, with the amplitude of input signals are within the interval $[r_a, r_b]$

III. SYMMETRIC AND UNIFORM SIGNAL DECOMPOSED POWER AMPLIFIER

A. DECOMPOSE ALGORITHM

We firstly introduce the detailed decompose algorithm from high PAPR signal to multiple low PAPR branched signals in SUSDPA system. To reduce the fluctuation of the peak value and make it close to the average, we propose this algorithm which is appropriate for the situation of using multiple identical amplifiers with the same saturation power. What's more, this kind of symmetrical decomposed algorithm has low complexity. In order to study the best performance of our signal decomposed method, the distribution of η_i is given in Fig. 5(a) and Fig. 5(b).

1) WHEN THE NUMBER OF BRANCH n IS EVEN

As Fig. 5(a) shows, the distribution of η_i satisfies:

$$\eta_{2m} = \eta^*_{2m-1}, \quad m = 1, 2, \ldots, \frac{n}{2}. \tag{18}$$

Combining Eq.(18) with Eq.(2), we can obtain

$$\begin{cases} |\eta_{2m}| = |\eta_{2m-1}| = \dfrac{1}{\sqrt{n}}; \\ \theta_{2m} = -\theta_{2m-1}; \\ (|\eta_{2m}| cos\theta_{2m} + |\eta_{2m-1}| cos\theta_{2m-1}) \dfrac{n}{2} = 1, \end{cases} \tag{19}$$

where θ_i is the phase of η_i, $i = 1, 2, \ldots, n$.

We acquire the distribution ratio η_i by solving Eq.(19), where j denotes imaginary symbol:

$$\begin{cases} \eta_i = \dfrac{1}{\sqrt{n}} exp[j(-arccos\dfrac{1}{\sqrt{n}})] & i = 1, 3, \ldots, n-1 \\ \eta_i = \dfrac{1}{\sqrt{n}} exp[j(arccos\dfrac{1}{\sqrt{n}})] & i = 2, 4, \ldots, n. \end{cases} \tag{20}$$

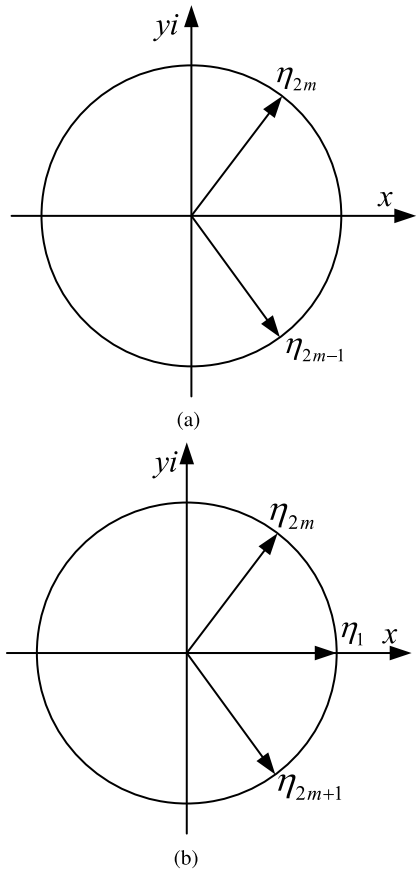

FIGURE 5. The Decompose Algorithm. (a) even branches decomposition. (b) odd branches decomposition.

2) WHEN THE NUMBER OF BRANCH *n* IS ODD

The distribution of η_i satisfy Fig. 5:

$$\begin{cases} \eta_1 = \dfrac{1}{\sqrt{n}} \\ \eta_{2m} = \eta^*_{2m+1}. \end{cases} \tag{21}$$

The similar procedure may be easily adapted to obtain the solution when n is odd, so we give the final results as the following:

$$\begin{cases} \eta_i = \dfrac{1}{\sqrt{n}} exp[j(-arccos\dfrac{1}{\sqrt{n}})] & i = 3, 5, \ldots, n-1 \\ \eta_i = \dfrac{1}{\sqrt{n}} exp[j(arccos\dfrac{1}{\sqrt{n}})] & i = 2, 4, \ldots, n \\ \eta_1 = \dfrac{1}{\sqrt{n}} & i = 1. \end{cases} \tag{22}$$

B. DECOMPOSITION METHOD BASED ON SIGNAL STATISTICS

Having determined the decompose algorithm, we can decompose the high PAPR signal into multiple low PAPR branched-signals. However, some signals may not belong to high PAPR signal. If the same algorithm is used for all original signals, with the process of the reduction of high power signal, the low power signal will be lowered in the branch as well. It means that each branched-signal is the scaling of the original signal, which is impossible to decrease the PAPR. Hence, we must adopt different decomposition algorithms for the signals with different amplitudes.

We take the SUSDPA system with 3 branched-signals as an example. The powers of input signals are determined by the saturation powers of branched-PAs. Hence, we take the saturation amplitudes of branched-PAs as standards, and classify the original signals $x(t)$ into small signals, medium signals and large signals based on their different instantaneous amplitudes $r(T)$, where T belongs to the OFDM symbol duration.

We denote the ith branched signal after decomposition as $x_i(t)$, and denote the saturation power of the ith branched-PA as V_i^2. The decomposition method is given as follows:

1) SMALL SIGNAL

If $r(T) < V_1$, we employ the 1st branched amplifier to satisfy the amplification requirement. In this case, the signal with small power does not need to be decomposed. According to Eq.(22), $n = 1$ and $x_i = \eta_i x$, we obtain the decomposed equations set:

$$\begin{cases} x_1(t) = x(t) \\ x_2(t) = 0 \\ x_3(t) = 0. \end{cases} \tag{23}$$

2) MEDIUM SIGNAL

If $V_1 < r(T) \leq \sqrt{V_1^2 + V_2^2}$, the instantaneous power is larger than the saturation power of the 1st branch amplifier. Thus, we employ both the 1st and 2nd branched amplifiers to decompose the original signal into two branched signals. Substituting $n = 2$ into Eq.(20) and according to $x_i = \eta_i x$, the final decomposed equations set is

$$\begin{cases} x_1(t) = (0.5 + 0.5j)x(t) \\ x_2(t) = (0.5 - 0.5j)x(t) \\ x_3(t) = 0. \end{cases} \tag{24}$$

3) LARGE SIGNAL

If $r(T) > \sqrt{V_1^2 + V_2^2}$, the instantaneous power is larger than the saturation power of the combined 1st and 2nd branched amplifiers. In this case, we have to decompose the original signal into 3 branched signals, which needs 3 amplifiers. Substituting $n = 3$ into Eq.(22) and according to $x_i = \eta_i x$, we obtain the decomposed equations as

$$\begin{cases} x_1(t) = (0.2113 + 0.5373j)x(t) \\ x_2(t) = (0.2113 - 0.5373j)x(t) \\ x_3(t) = 0.5774x(t). \end{cases} \tag{25}$$

A three-branched-signals decomposed structure is shown in Fig. 6. To sum up, rearranging Eq. (23)-(25), the 1st branched-signal $x_1(t)$ can be described as

$$x_1(t) = \begin{cases} x(t) & r(T) < V_1 \\ (0.5 + 0.5j)x(t) & V_1 < r(T) \leq \sqrt{V_1^2 + V_2^2} \\ (0.2113 + 0.5373j)x(t) & r(T) > \sqrt{V_1^2 + V_2^2}. \end{cases} \tag{26}$$

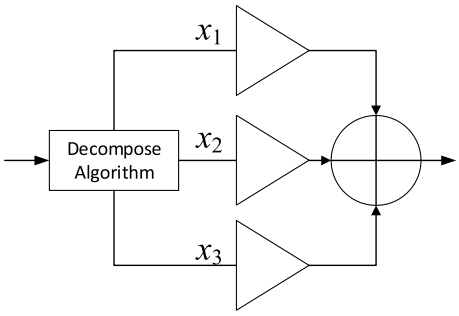

FIGURE 6. Three-Branched-Signals Structure.

Similar to $x_1(t)$, $x_2(t)$ and $x_3(t)$ can be described respectively as follows,

$$x_2(t) = \begin{cases} 0 & r(T) < V_1 \\ (0.5 - 0.5j)x(t) & V_1 < r(T) \le \sqrt{V_1^2 + V_2^2} \\ (0.2113 - 0.5373j)x(t) & r(T) > \sqrt{V_1^2 + V_2^2}, \end{cases} \tag{27}$$

$$x_3(t) = \begin{cases} 0 & r(T) < V_1 \\ 0 & V_1 < r(T) \le \sqrt{V_1^2 + V_2^2} \\ 0.5774x(t) & r(T) > \sqrt{V_1^2 + V_2^2}. \end{cases} \tag{28}$$

The original signal has been decomposed into 3 branch signals. According to the differences of signal distribution densities, x_1, x_2 and x_3 are termed as the High Density Signal (HDS), Medium Density Signal (MDS) and Low Density Signal (LDS) respectively, as Fig. 7 shows. With our algorithm and decomposition method, we can make the best PAPR performance for the situation of using multiple identical amplifiers. To find the best PAPR performance out, $V_1 = V_2 = V_3$ is assumed in the parts of PAPR analysis and the simulation. The calculation of PAPR decrease for HDS, MDS and LDS will be given in the following section.

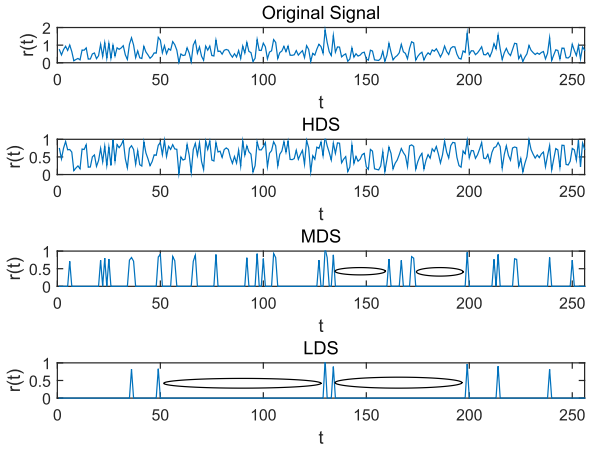

FIGURE 7. The amplitude of original Signal, HDS, MDS and LDS.

C. PAPR ANALYSIS OF BRANCHED SIGNALS

According to the above-mentioned hypothesis that the peak power of the original x is $POW_{max} = max|x(T)|^2$, where T belongs to the OFDM symbol duration, the PAPR of the original signal can be defined as

$$PAPR = 10log_{10}\frac{POW_{max}}{E\{x^2\}}. \tag{29}$$

According to **Lemma 1**, the probability of OFDM signals within the interval $(r_a, r_b]$ is

$$P(0, V_1) = [-exp(\frac{-r^2}{2\sigma^2})]_{r_a}^{r_b} \tag{30}$$

Since the amplitude of the input signal is segmented into three intervals, i.e., $(0, V_1]$, $(V_1, \sqrt{V_1^2 + V_2^2}]$ and $(\sqrt{V_1^2 + V_2^2}, +\infty)$ respectively, we can obtain the probability of OFDM signals on each intervals.

$$\begin{cases} P_1 = vP(0, V_1) = [1 - exp(\frac{-V_1^2}{2\sigma^2})], \\ P_2 = P(V_1, \sqrt{V_1^2 + V_2^2}) = [exp(\frac{-V_1^2}{2\sigma^2}) - exp(\frac{-(V_1^2 + V_2^2)}{2\sigma^2})], \\ P_3 = P(\sqrt{V_1^2 + V_2^2}, +\infty) = [exp(\frac{-(V_1^2 + V_2^2)}{2\sigma^2})]. \end{cases} \tag{31}$$

Next, the average power $E\{x^2\}$ satisfy the following equation:

$$E\{x^2\} = (POW_1 + POW_2 + POW_3), \tag{32}$$

where POW_1,POW_2 and POW_3 denote the average powers of small, medium and large signal respectively. Then, according to **Lemma 2** we can straightforwardly obtain

$$\begin{cases} POW_1 = [2\sigma^2 - (V_1^2 + 2\sigma^2)exp(\frac{-V_1^2}{2\sigma^2})], \\ POW_2 = [(V_1^2 + 2\sigma^2)exp(\frac{-V_1^2}{2\sigma^2}) \\ \qquad - (V_1^2 + V_2^2 + 2\sigma^2)exp(\frac{-(V_1^2 + V_2^2)}{2\sigma^2})], \\ POW_3 = (V_1^2 + V_2^2 + 2\sigma^2)exp(\frac{-(V_1^2 + V_2^2)}{2\sigma^2}). \end{cases} \tag{33}$$

The PAPR decrease of each branched-signals can be deduced by using the above formulas.

For the HDS x_1, the power of small signal remains unchanged. The average power of the signals belonging to small signal is POW_1. According to **Lemma 3**, the power of the medium signal becomes half of the original medium signal, thus the average power of the signals that belongs to medium signal is $POW_2/2$ calculated by Eq.(9). Similarly, the power of the large signal becomes one third of the original large signal, thus the average power of all the signals belonging to large signal is $POW_3/3$, while the peak signal becomes 1/3 of the original peak signal as well. Hence, we obtain the following formula

$$POW_{HDS} = POW_1 + \frac{1}{2}POW_2 + \frac{1}{3}POW_3. \tag{34}$$

Then, compared to the PAPR of original signals, the deduction of PAPR of the HDS, i.e., $\Delta PAPR_{HDS}$, could be expressed as

$$\begin{aligned}\Delta PAPR_{HDS} &= PAPR - PAPR_{HDS} \\ &= 10log_{10}\frac{3(POW_1+\frac{1}{2}POW_2+\frac{1}{3}POW_3)}{POW_1+POW_2+POW_3}.\end{aligned} \tag{35}$$

Since all the parameters in Eq.(35) is readily calculated, we can straightforwardly acquire the decreasing amount of PAPR of the HDS.

In the MDS x_2, the small signal does not exist, and the rest of signals will form a new signal to calculate the average power. In this case, the medium signal and large signal are 1/2 and 1/3 of the original signal respectively, as Fig. 7 (MDS) shows. We could get the average power of MDS:

$$POW_{MDS} = \frac{1}{2}POW_2 + \frac{1}{3}POW_3 \tag{36}$$

However, the small signal disappears in MDS signal after decomposition, meaning that there exists a lot of zero signals in MDS signal, as Fig. 7 (MDS) shows. In reality, One of the disadvantages of high PAPR signals is that different signals will be amplified in different level by PA, which significantly increases the BER in the receiver. However, zero signals cannot be magnified by PA, which means zero signals cannot effect the system performance and need not to be considered in PAPR calculation. Without considering the zero signals, the rest signal of MDS can be considered to form a new signal $S(MDS)$, as Fig. 8 (S(MDS)) shows. From Eq. (12) we have

$$POW(S_{MDS}) = \frac{POW_{MDS}}{P(V_1, +\infty)}. \tag{37}$$

Therefore, we can similarly calculate the decreased amount of PAPR of the MDS, i.e., $\Delta PAPR_{MDS}$ as,

$$\begin{aligned}\Delta PAPR_{MDS} &= PAPR - PAPR_{MDS} \\ &= 10log_{10}\frac{\frac{3}{2}POW_2+POW_3}{(P_2+P_3)(POW_1+POW_2+POW_3)}.\end{aligned} \tag{38}$$

Eq. (38) is the calculation formula for the decreasing amount of PAPR of the MDS.

In the LDS x_3, both the medium and small signals are not existed any more, and the rest signals will also form a new signal to calculate the average power. Meanwhile, there is only the large signal, whose power becomes 1/3 of the original signal. Hence, the following formulas are obtained:

$$POW_{LDS} = \frac{1}{3}POW_3 \tag{39}$$

and

$$POW(S_{LDS}) = \frac{POW_{LDS}}{P(\sqrt{V_1^2+V_2^2}, +\infty)}. \tag{40}$$

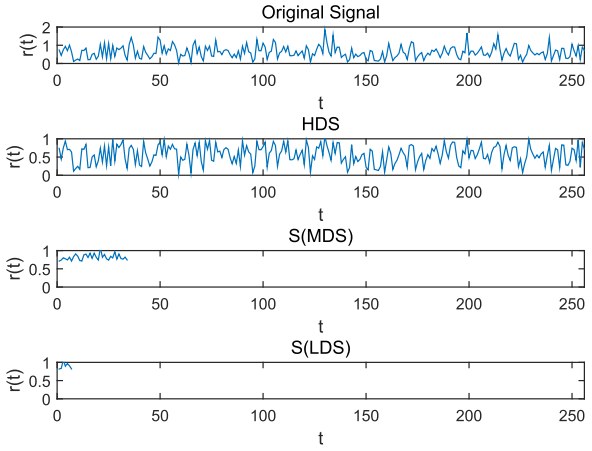

FIGURE 8. The amplitudes of original Signal, HDS, S(MDS) and S(LDS).

Similar to the MDS, the PAPR decrease can be deduce as

$$\begin{aligned}\Delta PAPR_{LDS} &= PAPR - PAPR_{LDS} \\ &= 10log_{10}\frac{POW_3}{P_3(POW_1+POW_2+POW_3)}.\end{aligned} \tag{41}$$

Eq. (41) gives the decreased amount for the PAPR of the LDS. Till now, we have provided the decreasing amount for PAPR of the three branched signals according to Eq. (35), Eq. (38) and Eq. (41). It is obvious that the PAPRs of all the three branched signals decrease dramatically.

D. POWER EFFICIENCY ANALYSIS

In this subsection, the power efficiency of PA will be analyzed. PA adopts the linear model as Figure 3 shows. We take the system with 3 branched-signals as an example and assume the saturation power of branched-PA are V_1^2, V_2^2 and V_3^2 respectively, which are same as section III-B.

Since the signal is separated in different intervals, we could also discuss the power efficiency in intervals respectively. From Eq. (33), POW_1, POW_2 and POW_3 could be calculated. As Eq. (16) shows, δ_{HDS} can be deduced as

$$\begin{aligned}\delta_{HDS} &= \frac{POW_{HDS}}{2V_1^2} \\ &= \frac{POW_1}{2V_1^2} + \frac{POW_2}{4V_1^2} + \frac{POW_3}{6V_1^2}.\end{aligned} \tag{42}$$

For MDS and LDS, the power efficiency δ_{MDS} and δ_{LDS} can be expressed as follows:

$$\begin{cases}\delta_{MDS} = \dfrac{POW_{MDS}}{2V_2^2} \\ \delta_{LDS} = \dfrac{POW_{LDS}}{2V_3^2}\end{cases} \tag{43}$$

However, there exists lots of zero number signals in the MDS and LDS, as is shown in Fig. 7. That is to say, branched-PA could be closed when the input signal equals to zero, which will remarkably increase the power efficiency of branched-PA.Without considering the zero signals, from

Eq. (17), the power efficiency of δ_{MDS} and δ_{LDS} should be deduced as follows:

$$\begin{cases} \delta_{MDS} = \dfrac{POW_{MDS}}{2V_2^2 P(V_1, \sqrt{V_1^2 + V_2^2})}, \\ \delta_{LDS} = \dfrac{POW_{LDS}}{2V_3^2 P(\sqrt{V_1^2 + V_2^2}, \sqrt{V_1^2 + V_2^2 + V_3^2})}. \end{cases} \tag{44}$$

Considering the power loss caused by power combiner, the practical power efficiency maybe lower than Eq. (42) and (44). With the latest technology [32]–[35], the power loss due to power combiner will not be more than 1dB, and the total combination efficiency can achieve 94.5%. Hence, we can assume that the power loss due to power combiner is 1dB (less than it in practice). Then the power efficiency is approximately 0.891 of that calculated by Eq. (42) and (44).

Since both of $P(V_1, \sqrt{V_1^2 + V_2^2})$ and $P(\sqrt{V_1^2 + V_2^2}, \sqrt{V_1^2 + V_2^2 + V_3^2})$ are smaller than 1, the power efficiency could be increased, which will be proved via simulation in section IV.

IV. SIMULATION RESULTS

In this section, the PAPR performance and power efficiency of the proposed scheme are evaluated by simulation experiments. The PAPR of the discrete-time signal is defined as Eq. (29) with the purpose of comparison of PAPR.

In general, the performance of PAPR is usually evaluated with the complementary cumulative distribution function (CCDF), whose definition is

$$CCDF_{PAPR(x)} = Prob(PAPR(x) > D). \tag{45}$$

$Prob(PAPR(x) > D)$ means the probability that $PAPR(x)$ is greater than a certain threshold value D.

A. SIMULATION CONDITION

In this section, we employ the OFDM system with 256 subcarriers in the simulation, whose mapping mode utilizes the normalized 16QAM squareness. The model used in this amplifier is the ideal linear amplification model, whose power gain is $G = 1$. The three-branched-model is used in this SUSDPA system, and the saturation power of branched-amplifier can be assumed as $V_1^2 = V_2^2 = V_3^2 = 1$ because the power of original OFDM signal is normalized in the simulation. The decomposition algorithm is same as Eq.(26), Eq. (27) and Eq. (28).

B. COMPARISON OF THE CCDF

In the subsection, we choose OFDM, T-OFDM [13] and precode OFDM [14] for comparison, which are marked as OFDM, T-OFDM and Precode respectively in Fig. 9. After decomposing the high PAPR signal by the SUSDPA, the results in Fig. 9 show the CCDF of all the decomposed branched signals.

It can be seen that the PAPR of OFDM remains comparatively high. According to [16], the PAPR values of the transmitted signal in the T-OFDM system are less than that of the OFDM system by a range of 0.75∼ 1.2 dB. However, with the method of this paper, the PAPRs of all the decomposed signals are decreasing dramatically, where the decreasing amounts of the HDS, MDS and LDS are approximately 3.8dB, 6.4dB and 7.2dB respectively. From Fig. 9 we could also find that, compared to other schemes, the PAPR of MDS and LDS decreases remarkably, which means the branched signals of SUSDPA have better PAPR performance.

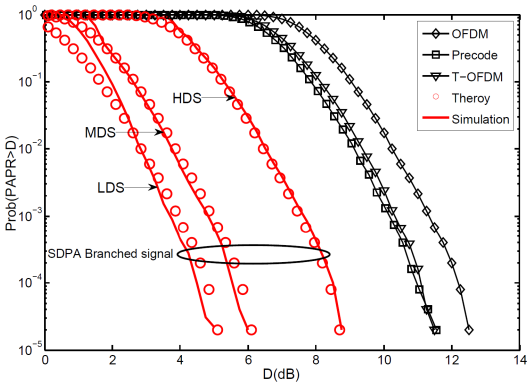

FIGURE 9. The performance of PAPR reduction of various system.

Moreover, a good estimation of the power density of the conventional OFDM, T-OFDM and SUSDPA systems can be acquired from the histograms plot of the peak power of such systems, as shown in Fig. 10. In terms of the OFDM and T-OFDM, the overall probability density function (PDF) of the T-transform can be approximated as Gaussian and the peak of the T-OFDM system is closer to that of the OFDM system, and the performance of T-OFDM is slightly better than OFDM. As is clear in this figure, variance changes of the HDS, MDS and LDS peaks are smaller than that of the T-OFDM and conventional OFDM. Fig. 10 also clearly shows how the SUSDPA system outperforms OFDM and T-OFDM by having the fewest signals with high peaks, i.e., lower PAPR.

C. COMPARISON OF THE POWER EFFICIENCY

Since $V_1^2 = V_2^2 = V_3^2 = 1$ is adopted in this simulation, for fairness we choose a equivalent WR-PA with saturation point $V_{WR}^2 = 3$ in other system for comparison, i.e., SCFDE, OFDM and Precoded OFDM.

In high PAPR system, power efficiency is a huge problem because of the nonlinear and saturation distortion of PA. Therefore, the output power of PA has to be backed off, which remarkably decreases the power efficiency of PA. In the SUSDPA system, we have no need to conduct OBO since the PAPR of each branched signal has decreased, which avoids energy waste and increases the power efficiency of branched PA. Moreover, we can utilize the amplifier with small operating point at small dynamic range to amplify the signal because the peak power of branched signal have also decreased, which straightforwardly decreases energy waste

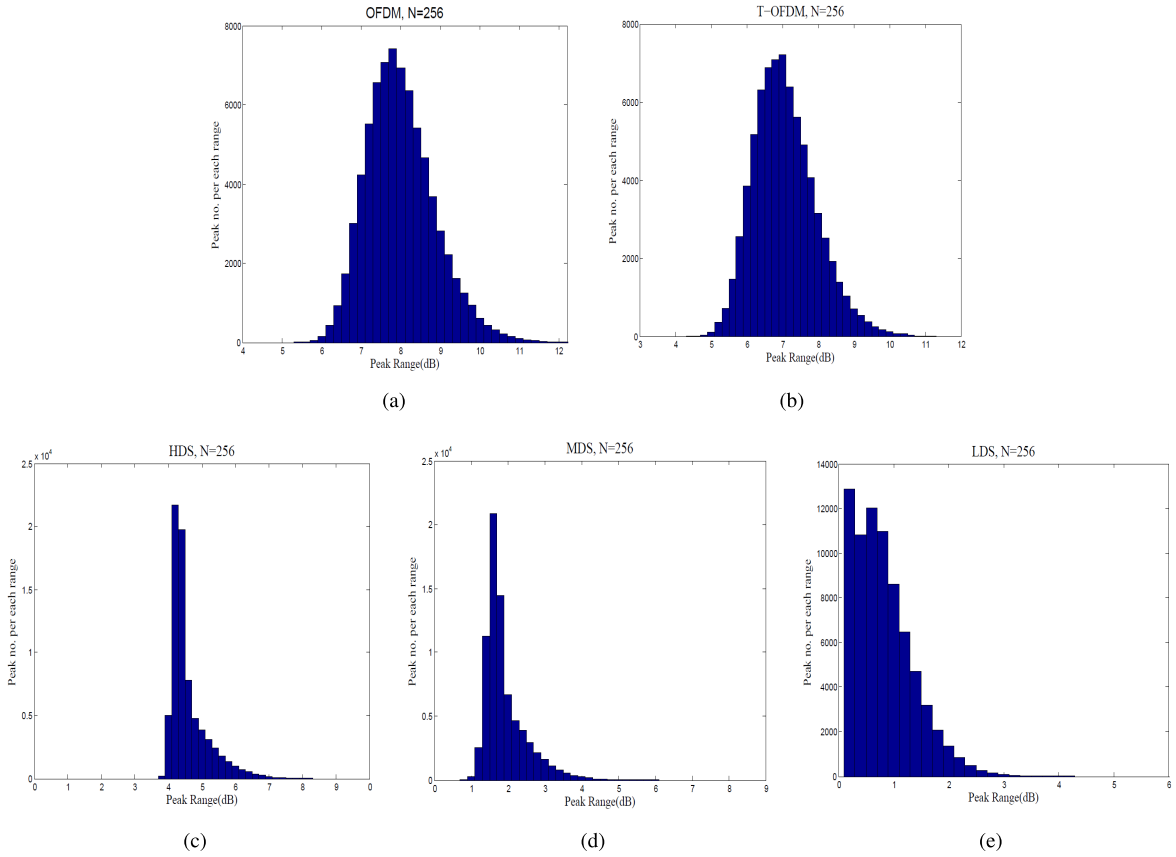

FIGURE 10. Histogram for peak power of the conventional OFDM, T-OFDM and SUSDPA systems (N=256). (X-axis represents the peaks range in dB and Y-axis represents the number of peaks that equal to each range in X-axis.)

TABLE 2. The comparison of power efficiency.

System	Power Efficiency	Power Efficiency theoretical
HDS PA	22.8%	23.9%
MDS PA	32.6%	32.7%
LDS PA	35.8%	40.7%
OFDM	14.9%	/
SCFDE	16.6%	/
Precoded OFDM	15.8%	/

and improves the power efficiency as well. More importantly, the MDS PA and LDS PA will be closed when the input signal equals to zero, which would significantly increase the power efficiency too.

As Table 2 shows, the power efficiency of HDS PA, MDS PA and LDS PA are all higher than traditional OFDM system. Especially, the power efficiency of MDS PA and LDS PA reaches 32.6% and 35.8% respectively, which is nearly 18% and 21% higher than OFDM system respectively.

D. COMPARISON OF THE COMPLEXITY

The result of complexity of Precoded OFDM, T-ofdm and SCFDE have been analyzed in [14]. In this subsection, the complexity of SUSDPA will be analyzed and compared with other schemes.

TABLE 3. Transmitter.

System	Num. of Complex Multip.	Num. of Complex Add.
SUSDPA	N	N
T-OFDM	$\frac{N}{2}log_2(N)-(N-1)$	$\frac{3N}{2}log_2(N)-3(N-1)$
Precoded OFDM	0	$3N$
SCFDE	0	0

TABLE 4. Receiver.

System	Num. of Complex Multip.	Num. of Complex Add.
SUSDPA	$Nlog_2(N)+N$	$2Nlog_2(N)$
T-OFDM	$\frac{N}{2}log_2(N)+N$	$\frac{N}{2}log_2(N)+N(N-1)$
Precoded OFDM	$Nlog_2(N)+N$	$2Nlog_2(N)+3N$
SCFDE	$Nlog_2(N)+N$	$2Nlog_2(N)$

In the transmitter of SUSDPA, as Eq. (20) and Eq. (22) shows, there is N complex multiply in signal decomposition period and N complex addition in signal combination period. Therefore, the comparison of complexity is shown in Table 3. The results indicate that SCFDE has the lowest complexity among these schemes, and the SUSDPA has low complexity than T-OFDM and Precoded OFDM in the transmitter.

In the receiver, since there is no extra operation in SUSDPA scheme, its complexity is similar to the SCFDE, as Table 4 shows, and lower than T-OFDM and Precoded OFDM. In conclusion, the complexity of SUSDPA is lower than T-OFDM and Precoded OFDM.

V. CONCLUSION

This paper has proposed a method for signal decomposition and amplification, which can satisfy the requirement of high efficiency amplifiers in the development of future communication system. The method employs the theory of signal decomposition and decomposes the high PAPR signal into multiple low PAPR branched signals. Then, the branched signals are amplified to decrease the power waste and increase the power efficiency, which is suitable for the development of green wireless communication network.

REFERENCES

[1] J. G. Andrews *et al.*, "What will 5G be?" *IEEE J. Sel. Areas Commun.*, vol. 32, no. 6, pp. 1065–1082, Jun. 2014.

[2] P. Pirinen, "A brief overview of 5G research activities," in *Proc. Int. Conf. 5G Ubiquitous Connectivity (5GU)*, Levi, Finland, Nov. 2014, pp. 17–22.

[3] M. Fiorani *et al.*, "Challenges for 5G transport networks," in *Proc. IEEE Int. Conf. Adv. Netw. Telecommun. Syst. (ANTS)*, New Delhi, India, Dec. 2014, pp. 6–8.

[4] R. Yoshizawa and H. Ochiai, "Trellis-assisted constellation subset selection for PAPR reduction of OFDM signals," *IEEE Trans. Veh. Technol.*, vol. 66, no. 3, pp. 2183–2198, Mar. 2017.

[5] Z. Zheng and G. Li, "An efficient FPGA design and performance testing of the ACE algorithm for PAPR reduction in DVB-T2 systems," *IEEE Trans. Broadcast.*, vol. 63, no. 1, pp. 134–143, Mar. 2017.

[6] X. Cheng, D. Liu, S. Feng, H. Fang, and D. Liu, "An artificial bee colony-based SLM scheme for PAPR reduction in OFDM systems," in *Proc. IEEE Int. Conf. Comput. Intell. Appl. (ICCIA)*, Beijing, China, Dec. 2017, pp. 449–453.

[7] V. Vahidi and E. Saberinia, "OFDM high speed train communication systems in 5G cellular networks," in *Proc. IEEE Annu. Consum. Commun. Netw. Conf. (CCNC)*, Las Vegas, NV, USA, Jan. 2018, pp. 1–6.

[8] G.-R. Lee, C.-H. Cheng, and H.-L. Hung, "Selected mapping applied scheme for PAPR reduction in OFDM communication systems," in *Proc. Int. Conf. Netw. Comput. Adv. Inf. Manage.*, Seoul, South Korea, Aug. 2010, pp. 752–755.

[9] S. Y. L. Goff, B. K. Khoo, C. C. Tsimenidis, and B. S. Sharif, "A novel selected mapping technique for PAPR reduction in OFDM systems," *IEEE Trans. Commun.*, vol. 56, no. 11, pp. 1775–1779, Nov. 2008.

[10] L. Yang, K. K. Soo, Y. M. Siu, and S. Q. Li, "A low complexity selected mapping scheme by use of time domain sequence superposition technique for PAPR reduction in OFDM system," *IEEE Trans. Broadcast.*, vol. 54, no. 4, pp. 821–824, Dec. 2008.

[11] M. M. Rahman, M. N. Al Safa Bhuiyan, M. S. Rahim, S. Ahmed, and D. Das, "On the comparative performance of PAPR reducing phase sequences for OFDM system," in *Proc. IEEE Region 10 Humanitarian Technol. Conf. (R10-HTC)*, Dec. 2017, pp. 234–237.

[12] X.-G. Xia, "Precoded and vector OFDM robust to channel spectral nulls and with reduced cyclic prefix length in single transmit antenna systems," *IEEE Trans. Commun.*, vol. 49, no. 8, pp. 1363–1374, Aug. 2001.

[13] S. Wang, S. Zhu, and G. Zhang, "A Walsh-Hadamard coded spectral efficient full frequency diversity OFDM system," *IEEE Trans. Commun.*, vol. 58, no. 1, pp. 28–34, Jan. 2010.

[14] S.-H. Wang, C.-P. Li, K.-C. Lee, and H.-J. Su, "A novel low-complexity precoded OFDM system with reduced PAPR," *IEEE Trans. Signal Process.*, vol. 63, no. 6, pp. 1366–1376, Mar. 2015.

[15] M.-J. Hao and C.-H. Lai, "Precoding for PAPR reduction of OFDM signals with minimum error probability," *IEEE Trans. Broadcast.*, vol. 56, no. 1, pp. 120–128, Mar. 2010.

[16] M. S. Ahmed, S. Boussakta, B. S. Sharif, and C. C. Tsimenidis, "OFDM based on low complexity transform to increase multipath resilience and reduce PAPR," *IEEE Trans. Signal Process.*, vol. 59, no. 12, pp. 5994–6007, Dec. 2011.

[17] S. Kousai and A. Hajimiri, "An octave-range watt-level fully integrated CMOS switching power mixer array for linearization and back-off efficiency improvement," in *IEEE Int. Solid-State Circuits Conf. (ISSCC) Dig. Tech. Papers*, San Francisco, CA, USA, Feb. 2009, pp. 376–377.

[18] C. Tuna and D. L. Jones, "Tone injection with aggressive clipping projection for OFDM PAPR reduction," in *Proc. IEEE Int. Conf. Acoust., Speech Signal Process. (ICASSP)*, Mar. 2000, pp. 3278–3281.

[19] J. Hou, X. Zhao, F. Gong, F. Hui, and J. Ge, "PAPR and PICR reduction of OFDM signals with clipping noise-based tone injection scheme," *IEEE Trans. Veh. Technol.*, vol. 66, no. 1, pp. 222–232, Jan. 2017.

[20] W. Wang, M. Hu, J. Yi, H. Zhang, and Z. Li, "Improved cross-entropy-based tone injection scheme with structured constellation extension design for PAPR reduction of OFDM signals," *IEEE Trans. Veh. Technol.*, vol. 67, no. 4, pp. 3284–3294, Apr. 2018.

[21] W. Wang, M. Hu, Y. Li, and H. Zhang, "A low-complexity tone injection scheme based on distortion signals for PAPR reduction in OFDM systems," *IEEE Trans. Broadcast.*, vol. 62, no. 4, pp. 948–956, Dec. 2016.

[22] Y. Shirato and M. Muraguchi, "Signal decomposition technique for enhanced power added efficiency of OFDM transmitters and its application for MIMO systems," in *Proc. 46th Eur. Microw. Conf. (EuMC)*, Oct. 2016, pp. 146–149.

[23] Z. Ren, H. Zhang, and K. Guo, "A novel method for the improvement of power efficiency in high peak-to-average-power ratio communication systems," *Sci. China Inf. Sci.*, vol. 53, no. 8, pp. 1697–1702, 2010.

[24] Z. Hasan, H. Boostanimehr, and V. K. Bhargava, "Green cellular networks: A survey, some research issues and challenges," *IEEE Commun. Surveys Tuts.*, vol. 13, no. 4, pp. 524–540, 4th Quart., 2011.

[25] C.-L. I, C. Rowell, S. Han, Z. Xu, G. Li, and Z. Pan, "Toward green and soft: A 5G perspective," *IEEE Commun. Mag.*, vol. 52, no. 2, pp. 66–73, Feb. 2014.

[26] P. Jardin and G. Baudoin, "Filter lookup table method for power amplifier linearization," *IEEE Trans. Veh. Technol.*, vol. 56, no. 3, pp. 1076–1087, May 2007.

[27] Z. Ren and H. Zhang, "A novel distortion elimination method of power amplifier in wideband OFDM system," *Sci. China Inf. Sci.*, vol. 55, no. 2, pp. 396–406, 2012.

[28] X. Hong, S. Chen, Y. Gong, and C. J. Harris, "Nonlinear equalization of Hammerstein OFDM systems," *IEEE Trans. Signal Process.*, vol. 62, no. 21, pp. 5629–5639, Nov. 2014.

[29] X. Wu and J. Shi, "Adaptive Predistortion using cubic spline nonlinearity based Hammerstein modeling," *IEICE Trans. Fundam. Electron. Commun. Comput. Sci.*, vol E95-A, no. 2, pp. 542–549, 2012.

[30] H. Ochiai, "On power amplifier efficiencies of linearly modulated signals with nonlinear distortion," in *Proc. 8th Int. Symp. Wireless Commun. Syst. (ISWCS)*, Nov. 2011, pp. 397–401.

[31] F. H. Raab *et al.*, "Power amplifiers and transmitters for RF and microwave," *IEEE Trans. Microw. Theory Techn.*, vol. 50, no. 3, pp. 814–826, Mar. 2002.

[32] M. Gholami, R. E. Amaya, and M. C. E. Yagoub, "Low-loss compact power combiner for solid state power amplifiers with high reliability," *IET Microw., Antennas Propag.*, vol. 10, no. 3, pp. 310–317, Feb. 2016.

[33] R. Xiao, Y. Deng, Z. Song, J. Li, J. Sun, and C. Chen, "An all circular waveguide four-way power combiner with ultrahigh-power capacity and high combination efficiency," *IEEE Trans. Plasma Sci.*, vol. 46, no. 7, pp. 2475–2479, Jul. 2018.

[34] K. Chen, E. J. Naglich, Y.-C. Wu, and D. Peroulis, "Highly linear and highly efficient dual-carrier power amplifier based on low-loss RF carrier combiner," *IEEE Trans. Microw. Theory Techn.*, vol. 62, no. 3, pp. 590–599, Mar. 2014.

[35] C. Li and D. S. Ricketts, "A low-loss, impedance matched $\lambda/4$ compact T-junction power combiner," in *Proc. Microw. Integr. Circuits Conf.*, Oct. 2013, pp. 147–150.

ZHIYUAN REN received the M.S. and Ph.D. degrees in communication and information system from Xidian University in 2007 and 2011, respectively. He is currently an Associate Professor at the School of Telecommunication Engineering, Xidian University. He has published more than 20 journal publications and conference publications. His major research interests are distributed computing, mobile edge computing, and network virtualization in 5G.

ZEHUAN HU received the B.S. degree in communication engineering from the Xi'an University of Technology, Xi'an, China, in 2017. He is currently pursuing the M.S. degree in communications and information systems with Xidian University, Xi'an. His research interests include signal processing for wireless communications, MIMO and OFDM wireless communications, and network virtualization in 5G.

HAILIN ZHANG (M'97) received the B.S. and M.S. degrees from Northwestern Polytechnic University, Xian, China, in 1985 and 1988, respectively, and the Ph.D. degree from Xidian University, Xi'an, China, in 1991. In 1991, he joined the School of Telecommunications Engineering, Xidian University, where he is currently a Senior Professor and the Dean. He is also the Director of the Key Laboratory in Wireless Communications sponsored by the China Ministry of Information Technology, a Key Member of the State Key Laboratory of Integrated Services Networks, one of the state government specially compensated scientists and engineers, a field leader in telecommunications and information systems with Xidian University, and an Associate Director of the National 111 Project. He has published more than 150 papers in journals and conferences. His current research interests include key transmission technologies and standards on broadband wireless communications for 5G and 5G-beyond wireless access systems.